Contents lists available at ScienceDirect

Ocean Engineering

journal homepage: www.elsevier.com

The effect of local wake model on collision probability for risers subjected to current and random waves

Ping Fu*, Bernt J. Leira, Dag Myrhaug

Department of Marine Technology, Norwegian University of Science and Technology, NO-7491 Trondheim, Norway

ARTICLE INFO

Keywords:
Wake interference
Riser collision probability
Waves and current
Wake models
Drag force

ABSTRACT

The present paper provides a method to estimate the clearance between two flexible risers in tandem arrangement by taking into account the hydrodynamic wake interference when subjected to a current flow and a combined current plus waves flow. Modelling of the wake interference in the near wake field is based on the modification of the mean wake velocity deficit in the far wake field. Two modified wake models are introduced in the presented paper. The wake effects in a steady current and in current plus waves are investigated by using both wake models. For the current-only flow, the deflection shapes of a pair of tandem risers in steep-wave configuration are presented, highlighting the importance of the wake effect on clearance estimation. For combined current plus waves, the wake interference is investigated by considering the position-dependent drag force, for different combinations of riser natural frequency and wave frequency. The collision failure probability is predicted when the risers are subjected to current plus random waves.

1. Introduction

The collision between adjacent risers in an array has become an important issue as the oil and gas industry moves to deep water, since the risk of collision increases with increasing water depth. Potential collision can be caused by the wake interference, which takes place when the downstream cylinder is placed within the wake field generated by the upstream one. The wake interference will change the flow around the downstream riser, i.e., reducing the local flow velocity. This change will therefore reduce the drag force acting on the downstream riser, and induce an additional lift force if the risers are in staggered arrangement. This effect in turn reduces the clearance between the risers, leading to a potential clashing. One possible model for calculating the velocity deficit behind a single cylinder is given by Schlichting and Gersten (2003). This model expresses the velocity deficit as a function of the relative distance between the downstream and upstream cylinders, and gives good agreements with the experimental data in the far wake field. Huse et al. (1998, 2000) modified the model by introducing a concept of 'virtual source distance' so that the wake model can be applied in the near wake field. The authors also proposed a calculation procedure for predicting the drag reduction on individual cylinders in an array. Blevins (2005) developed a wake model by correlating experimental data with the Schlichting's wake model, which allows that both lift and drag forces can be determined in closed form in terms of the single cylinder drag coefficient, the relative distance between the two cylinders, and their diameters.

Wake interference might also cause instability problem for high value of the reduced velocity, i.e. Wake-Induced-Oscillation (WIO). It refers to the state that when the downstream cylinder is placed in the wake of the upstream one, any small disturbance to the system might force the downstream cylinder into an unstable state, i.e. a small disturbance can either be amplified until a new equilibrium state is achieved, or the system breaks and collision between the risers occurs (Wu, 2003). The mechanism of WIO is not yet fully understood, and research is ongoing (Hover and Triantafyllou, 2001; Huera-Huarte and Bearman, 2011; Huera-Huarte and Gharib, 2011; Huang et al., 2011; Huang and Herfjord, 2013). It is observed from the experiments that WIO is a low-frequency motion with large amplitude, arising at the first natural period of the riser which is substantially lower than the vortex shedding frequency. The oscillation amplitude is larger than 4D even when the reduced velocity exceeds the typical lock-in range. Huera-Huarte and Bearman (2011) investigated two flexible circular cylinders in the near wake with Reynolds number $R_e = VD/\nu$ up 12000 (where V is the flow velocity, D is the cylinder diameter and ν is the

* Corresponding author.
Email address: ping.fu@ntnu.no (P. Fu)

https://doi.org/10.1016/j.oceaneng.2018.04.099
Received 16 November 2017; Received in revised form 25 April 2018; Accepted 29 April 2018
Available online xxx
0029-8018/

kinematic viscosity), and found the different response regimes based on the type of oscillations exhibited by the cylinders: VIV (vortex-induced vibration), WIO or combinations of both. Moreover, Wu (2003) investigated the mechanism of WIO of a pair of tandem riser arrangements numerically. The author applied a full Routh-Hurwitz stability algorithm together with a direct numerical eigenvalue search technique for understanding the mechanism of WIO and prediction of potential collision.

Another reason for riser collision is the oscillating wave loads which can excite individual risers moving dynamically around the static equilibrium positions. On one hand, the differences in excitation force on neighbouring risers will cause large relative distance, leading to possible collision, especially when subjected to a severe sea state. On the other hand, the wake interference caused by oscillating waves is also a reason for the collision. However, relatively few experimental studies have been carried out regarding riser collision caused by oscillating wave loads. Bushnell et al. (1977) carried out laboratory tests to determine the flow interference effects between arrays of cylinders subjected to harmonic oscillating flow. Duggal and Niedzwecki (1993) studied the complex interaction between regular and random waves for a single flexible cylinder. They performed an experimental study of tandem riser pairs subjected to random waves in order to understand the dynamic response due to wake interference.

In order to avoid collision, clearance assessment is required. Generally, there are two different design strategies for riser collision assessment according to DNV-RP-F203 (2009). One is called 'No Collision Allowed', which means that riser collision is not allowed under normal, extreme or survival conditions. The problem is then reduced to determine the probability of the relative distance between risers over a given threshold value. Another one is 'Collision Allowed', indicating that infrequent collision may be allowed in some extreme conditions. Hence, assessment of structural interaction is further required. For the present study, the former design strategy will be considered.

The objective of this paper is to develop a simplified method to estimate the clearance between risers when subjected to currents and combined current plus waves, by which the wake effect is taking into account. Particular attention is given to a pair of flexible risers in a wave configuration. The risers are arranged in tandem, so that the lift force on the downstream riser can be neglected. Two modified wake models, i.e., the Blevins model and the Huse model, are presented and applied in the analysis. Due to the non-linearity of the collision problem, time domain simulation is necessary. The wake effect in waves is investigated by a 2D cylinder system, which is achieved by updating the drag coefficient at each time step based on the instantaneous relative position. The results are compared with that for the constant drag coefficient. In addition, collision probability between two cylinders subjected to current plus random waves is estimated.

2. Wake model

2.1. Mean deficit velocity

According to Schlichting and Gersten (2003) the local flow velocity behind a single cylinder can be expressed as the difference between the undistributed flow velocity, given as,

$$V(x,y) = V_0 - V_d(x,y) = V_0\left(1 - \hat{V}_d(x,y)\right) \tag{1}$$

where $V(x,y)$ is the local flow velocity in the wake field; V_0 is the free-stream current velocity; $V_d(x,y)$ is the mean deficit velocity, and $\hat{V}_d(x,y) = V_d(x,y)/V_0$ is the non-dimensional mean deficit velocity, which can be expressed as:

$$\hat{V}_d(x,y) = 0.95\sqrt{\frac{C_{D_0}D}{x}}\exp\left\{-\frac{y^2}{0.08888C_{D_0}Dx}\right\} \tag{2}$$

where C_{D_0} is the reference drag coefficient and D is the diameter of the cylinder. The origin of the local coordinate system is located at the center of the cylinder, with the x-axis pointing the incoming flow direction, and the y-axis in the transverse direction, as shown in Fig. 1.

Schlichting's formula agree well with experimental data in the far wake field, i.e. $x/D > 50$ (Schlichting and Gersten, 2003). However, in the near wake field, it gives too large velocity deficits and a too narrow wake, leading to an error when calculating the drag force on the downstream cylinder by using the Morison equation (Fredheim, 2005). Therefore, two modified models for calculation of the drag force in the near wake field are introduced.

2.2. Huse model

Huse et al. (2000) introduced a concept of 'virtual source distance', i.e. $x_v = 4D/C_D$, which means that the origin is moved to the front of the cylinder so that the wake width at the cylinder center is exactly equal to the cylinder diameter, see Fig. 2. Hence, the local flow velocity $\hat{V}_d(x,y)$ can be determined by using the modified distance $x_s = x + x_v$ instead of x in Eq. (2).

A problem is that the deficit velocity $V_d(x,y)$ varies over the domain occupied by the downstream cylinder. To solve this problem, Huse suggested that the root-mean-square (RMS) value averaged over the cylinder diameter, i.e. $V_{d,rms}(x,y)$, can be used for calculating the drag force, which in non-dimensional form in terms of V_0 is given by:

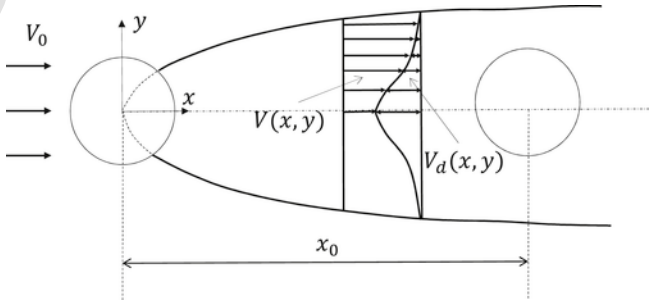

Fig. 1. Sketch of the Schlichting model.

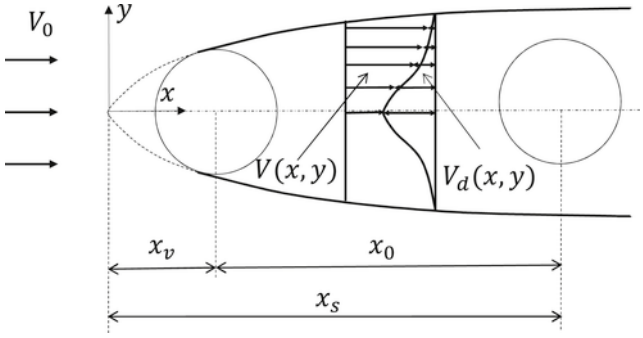

Fig. 2. Sketch of the Huse model.

$$\hat{V}_{d,rms}(x,y) = V_{d,rms}(x,y)/V_0 = \left\{ \frac{1}{D_2} \int_{y-\frac{D_2}{2}}^{y+\frac{D_2}{2}} \hat{V}_d^2(x,y)\, dy \right\}^{\frac{1}{2}} \quad (3)$$

where D_2 is the diameter of the downstream cylinder.

The drag force acting on the downstream cylinder can be calculated by the Morison equation as:

$$F_D = \frac{1}{2}\rho D_2 V_0^2 \left(1 - \hat{V}_{d,rms}\right)^2 C_{D0} \quad (4)$$

where ρ is the water density. The Huse model can easily be applied to a riser array by summing up the wake contributions from all upstream cylinders.

2.3. Blevins model

The Schlichting deficit velocity at the cylinder center is directly used in the Blevins model, with the assumption that the drag force on the downstream cylinder in the wake is proportional to the local dynamic pressure evaluated at its center. The variation of the local velocity can be translated to the variation of the drag coefficient by the expression:

$$\begin{aligned} F_D &= \frac{1}{2}\rho D_2 V^2(x,y) C_{D_0} \\ &= \frac{1}{2}\rho D_2 V_0^2 \left(1 - \hat{V}_d\right)^2 C_{D_0} \\ &= \frac{1}{2}\rho D_2 V_0^2 C_D(x,y) \end{aligned} \quad (5)$$

where

$$C_D(x,y) = C_{D0}\left(1 - \hat{V}_d\right)^2 \quad (6)$$

By inserting Eq. (2) into Eq. (6) it becomes:

$$C_D(x,y) = C_{D0}\left\{1 - k_1\left(\sqrt{\frac{C_{D_0} D_1}{x}}\right)\exp\left(\frac{-k_2 y^2}{C_{D_0} D_1 x}\right)\right\}^2 \quad (7)$$

where $k_1 = 1$ and $k_2 = 4.5$ are determined by fitting to the Price and Paidoussis (1984) experimental data at $x/D = 3$, 5, 9 and 20.3 by using the least-squares method according to Blevins (2005). However, more data is required in order to validate this model.

Blevins model also comprises the inward lift force on the downstream cylinder, towards the wake center-line, which is proportional to transverse gradient of drag, according to C. B. Rawlins' postulate. In the present study, however, the downstream riser is placed at the wake center-line so that the lift force caused by the asymmetry flow can be neglected; more details about the lift force induced by the wake effect are given in Blevins (2005).

2.4. Comparison and modification

In Figs. 3–6, the calculated drag coefficients obtained from the original Schlichting model and the modified Huse and Blevins models are presented, with different combinations of x/D and y/D. The reference

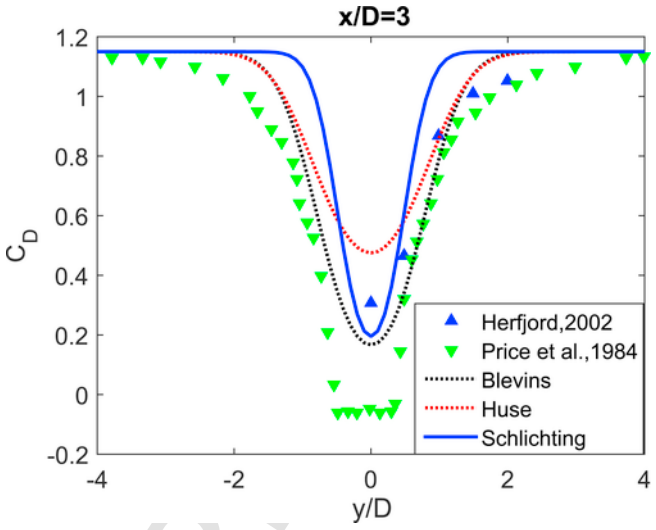

Fig. 3. Mean drag coefficient of the downstream cylinder for $x/D = 3$. ▲: Herfjord et al. (2002) for $R_e = 5.3\times10^4$; and ▼: Price and Paidoussis (1984) for $R_e = 5.3\times10^4$.

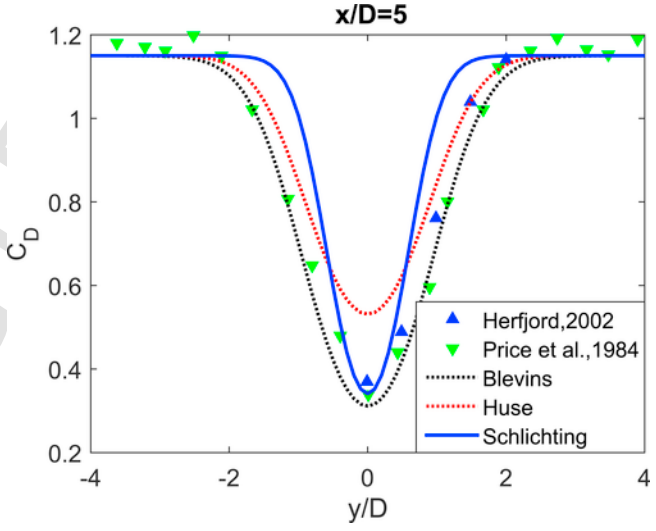

Fig. 4. Mean drag coefficient of the downstream cylinder for $x/D = 5$. ▲: Herfjord et al. (2002) for $R_e = 5.3\times10^4$; and ▼: Price and Paidoussis (1984) for $R_e = 5.3\times10^4$.

drag coefficient $C_{D_0} = 1.15$ is used for all the calculated results. In the same figure, the measurements by Price and Paidoussis (1984) and by Herfjord et al. (2002) for $R_e = 5.3\times10^4$ are presented. From Figs. 3 and 4 it appears that, compared with the original Schlichting model, the Huse model gives a wider wake and a smaller deficit velocity, resulting in a larger C_D in the tandem arrangement and a smaller C_D when the downstream cylinder is outside the wake center line. The Blevins model gives a wider wake but a smaller C_D due to the experimental data used for fitting.

Fig. 5 shows the calculated C_D for the three models versus horizontal distance x for $y = 0$. From the top figure, it appears that the models have the same asymptotic behaviour in the far wake field, i.e. $x \geq 50$. It also found that in the near wake field there are large differences between the Huse model and the other two models. The reason is that the origin in the Huse model (see Fig. 2) is not the same as in the other two models (see Fig. 1). The latter become singular at $x = 0$. Actually, the Blevins model is valid for a relative distance be-

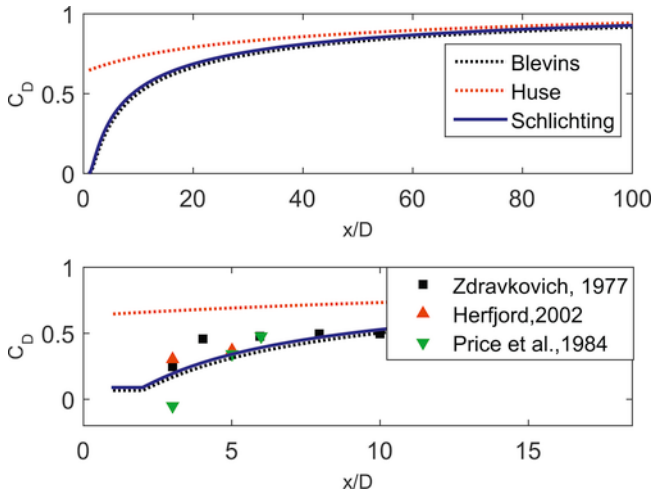

Fig. 5. Mean drag coefficient of the downstream cylinder for $y = 0$. ■: Zdravkovich (1977) for $R_e = 1.2\times10^5$; ▲: Herfjord et al. (2002) for $R_e = 5.3\times10^4$; and ▼: Price and Paidoussis (1984) for $R_e = 5.3\times10^4$.

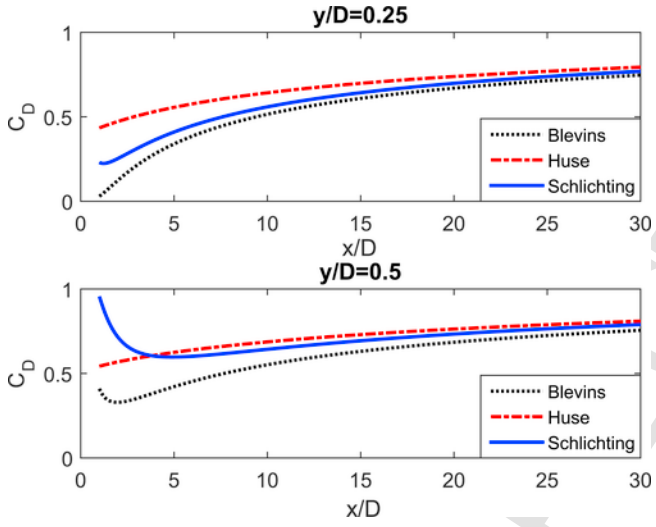

Fig. 6. Mean drag coefficient of the downstream cylinder using different models, with $y/D = 0.25$ (top) and 0.5 (bottom).

tween the centres of cylinders greater than 2–3 times the diameter of the upstream cylinder. At distances less than this value, the interference becomes more complex with negative suck force involved. To avoid this, it is assumed that the drag coefficient is constant if $x \le 2D$, and equal to the value of C_D at $x = 2D$. The modified model is shown in the bottom of Fig. 5. In the same figure, the measurements by Price and Paidoussis (1984) for $R_e = 5.3\times10^4$, by Zdravkovich (1977) for $R_e = 1.2\times10^5$, and by Herfjord et al. (2002) for $R_e = 5.3\times10^4$, are presented.

Fig. 6 presents the results for the different models as a function of x/D for $y/D = 0.25$ and $y/D = 0.5$, showing the properties of the modified models in the near wake. It appears that at $y/D = 0.25$, the Huse model always gives a larger C_D compared with the Blevins model; for $y/D = 0.5$, the difference between the two modified models becomes smaller, and C_D becomes larger, as a result of the wider wake.

For the upstream cylinder, Bokaian et al. (1985) has shown that the fluid interaction has no influence on the upstream cylinder if the relative distance is more than about 2–3 diameters. Thus, the drag force on the upstream cylinder is here calculated by the undisturbed Morison equation.

3. Wake interference in current

The wake effect in steady current is investigated by combining the finite element software RIFLEX (1987) along with the modified wake models. Riflex is specially designed to handle static and dynamic analyses of flexible risers and other slender structures. The static analysis methods comprise catenary analyses, available for a limited range of systems. The dynamic analysis comprises linear and nonlinear time domain analysis.

As mentioned previously, the drag force on the downstream riser depends on the wake models which are functions of the relative distance between downstream and upstream risers. Consequently,the forces vary along the risers due to the current profile and the riser boundary condition. In order to consider the wake interference in static analysis, an iteration procedure is necessary for determining the static equilibrium position. Particular attention is given to a pair of flexible risers with steep-wave configuration in tandem arrangement. A steep-wave riser has the addition of buoyancy modules along a part of the riser length in order to form a 'wave' shape, so that some of the axial tensile forces acting on the riser can be relieved, as shown in Fig. 7. The total length of the riser is $l = 160$ m with diameter $D = 0.25$ m. The length of the buoyancy module is $l_b = 50$ m with diameter $D_b = 0.63$ m, and along the riser at water depth $h = 60\sim90$ m. The main riser properties are summarized in Table 1.

Both Blevins model and Huse model are used in the static analysis. The iteration procedure is proposed in Fu et al. (2017). In the present

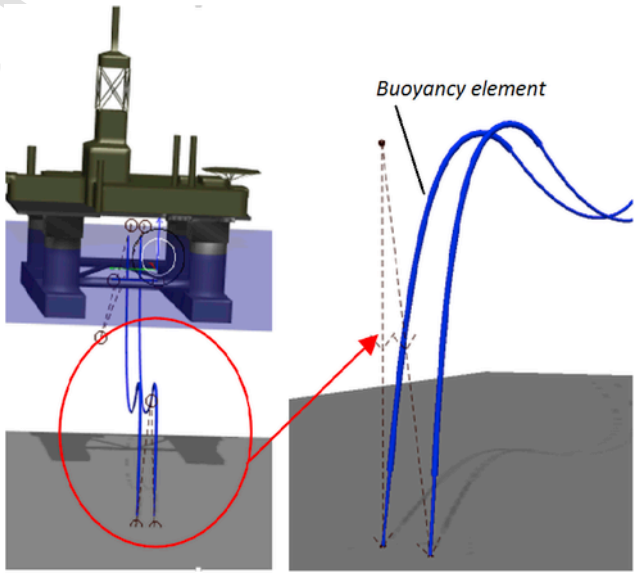

Fig. 7. Riser configuration.

Table 1
Riser and buoyancy elements properties.

	Unit	Riser	Buoyancy elements
Outside diameter	[m]	0.25	0.63
Inside diameter	[m]	0.05	0.05
Mass coefficient	[kg/m]	100	100
EI	[kNm^2]	104	104
Content density	[kg/m^3]	1000	1000
Total length	[m]	110	50

study, this method is refined by calculating the local drag force for each finite element instead of each segment. This is achieved by dividing the two risers into 320 elements and calculating the relative distance for each pair of elements.

The main steps used to determine the static equilibrium position are as follows:

1 Calculate the local drag coefficient, C_{D1} according to the Blevins model and the Huse model based on the initial position, i.e. L_0.
2. Perform a static analysis using Riflex and compute the relative distance between each pair of elements x_{ri}.
3 Update the local drag coefficient, i.e., C_{Di+1} based on the calculated distance x_{ri}.
4. Repeat steps 2–3 until convergence is achieved

The static equilibrium deflection shapes of the risers subjected to current loads are illustrated in Figs. 8 and 9 by using the different wake models, with different combinations of the current velocity V_0 and the initial center-to-center distance L_0. The finial deflection shapes of the two risers without wake effects are also shown in the same figures. The notation UR and DR in the figures refer to the upstream riser and downstream riser, respectively.

Fig. 8 presents the finial static deflection shape for initial distance $L_0 = 8m$ and current velocity $V_0 = 1m/s$. From the figure it appears that the wake effect has a notable influence on the downstream riser. Both of the modified models give a reduced relative distance, compared with that for the model with no wake effect. The minimum distance is identified in the joint region where the buoyancy modules and the bare riser segments are located. This is because the influence of the wake effect is significant in this region where the diameter and flexibility is increased. It is also observed that the Blevins model leads to a small gap at a submerged depth around $h = 60$ m where the relative distance $x_r = 1.8D$. Actually, in such close region, collision might happen due to the suck force in practice, depending on the Reynolds number and the roughness ratio (Zdravkovich, 1977).

In order to increase the final relative distance and avoid collision, some modifications can be carried out, as shown in Fig. 9. It is illustrated in Fig. 9a that the static equilibrium deflection shapes of risers when L_0 is increased from 8 m to 10 m. This change ensures that there is sufficient clearance between the upstream and downstream risers. In Fig. 9b the current velocity is decreased from 1.0 m/s to 0.8 m/s, which leads to a reduced drag force on the risers. As a consequence, the risk of riser collision can be reduced significantly.

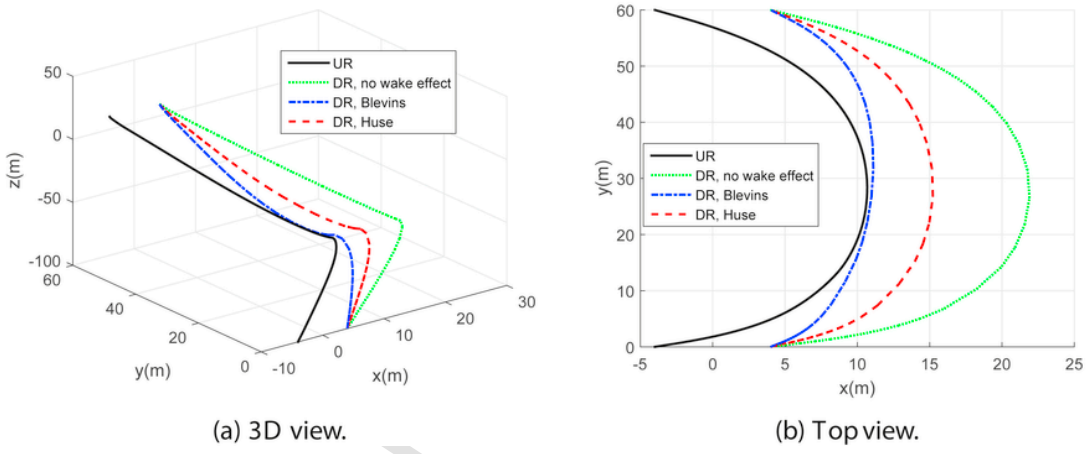

Fig. 8. Static deflection of flexile tandem risers under current loads calculated from different wake models, with $L_0 = 8m$ and $V_c = 1m/s$. (a) 3D view. (b) Top view. UR: upstream riser, DR: downstream riser.

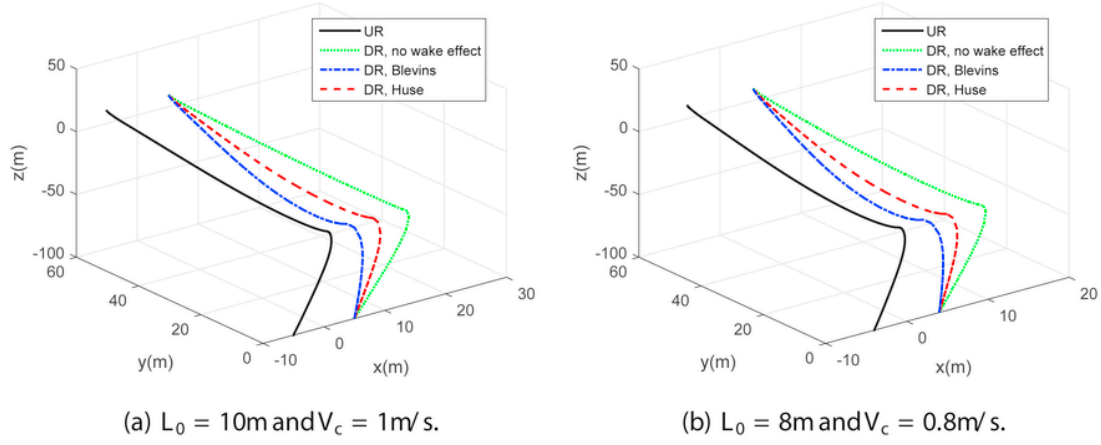

Fig. 9. Modified static deflection of flexible tandem risers under current loads calculated from different wake models. UR: upstream riser, DR: downstream riser.

4. Wake interference in current plus waves

4.1. Numerical model

Dynamic wave loads will excite the individual risers such that they oscillate around their static equilibrium positions. If the excitation corresponding to the fluid loads is so strong that the risers start to move with large amplitudes, the risers may collide with each other. The wave-induced excitation forces (Froude-Kriloff and diffraction forces) can be computed by a long wavelength approximation which involves added mass and potential damping of the actual cross section together with the wave kinematics. The viscous loads are computed using the drag term in a modified Morisons equation, taking into account the relative motion between risers and fluid flow. Additionally, wake effects generated by the upstream cylinder are accounted for in order to investigate the effect of the wake interference in waves. The hydrodynamic forces are calculated based on two-dimensional strip theory. In the present study, a simple 2D cylinder system with one degree of freedom is used, as shown in Fig. 10. Since the wake effects only influence the hydrodynamic behaviour of the downstream cylinder, and the configuration of the upstream cylinder does not change the property, the upstream cylinder is taken to be fixed in order to simplify the problem. The downstream cylinder is placed in the wake center-line and is free to oscillate in the x-direction, as illustrated in Fig. 10.

The equation of motion for the downstream cylinder in terms of the coordinate system $x' - y'$ can be written as:

$$\left(m + m_a\right)\ddot{x}' + c\dot{x}' + k\left(x_{20} + x'\right) = F_D + F_I \tag{8}$$

where the origin of the coordinate system (x', y') is placed at the center of the static position of the downstream cylinder, as shown in Fig. 10; m is the cylinder mass per unit length; m_a is the added mass per unit length; c is the structural damping; $F_I = C_m \rho D \ddot{x}$ is the inertia force per unit length; C_m is the inertia coefficient, and a typical value of 2 is used.

The drag force per unit length acting on the downstream cylinder is given by using the Morisons equation, taking into account the relative motion between the flow and the cylinder:

$$F_D = \frac{1}{2}\rho D V_r^* \left|V_r^*\right| C_D^* \tag{9}$$

where V_r^* is the relative velocity between the flow and the cylinder, and C_D^* is the drag coefficient. These parameters are defined as following according to different wake models.

1) V_r^* and C_D^* in the Huse model: Since the Huse model gives the local velocity as shown in Eq. (3), it is assumed that the drag coefficient of the downstream cylinder is the same as the upstream one, which is constant, i.e. $C_D^* = C_D$. This implies that the variation in the downstream cylinder's drag force will be governed by the local wake velocity. Considering the motion of the cylinders, V_r^* is defined as the relative velocity between the reduced flow and the moving cylinder, i.e. $V_r^* = \left(V_0 + V_w\right)\left(1 - \hat{V}_{d,rms}\right) - \dot{x}$, where V_w is the wave particle velocity. It is convenient to transfer the variation from the local wake velocity into a modified drag coefficient by introducing the following equality: $C_{D0} \cdot V_r^{*2} = C_D(x) \cdot \left(V_0 + V_w - \dot{x}\right)^2$.
2) V_r^* and C_D^* in the Blevins model: According to the Blevins model, the variation in the downstream cylinder's drag force is governed by the local drag coefficient as given in Eq. (7). The flow velocity is taken as the undisturbed velocity. Hence, the relative velocity V_r^* is defined as the relative velocity between the undisturbed flow and the moving cylinder, i.e. $V_r^* = V_0 + V_w - \dot{x}$.

The calculation of the drag force mentioned above is based on the assumption that the modified wake models, which have been established for steady flow, can be applied to a current-dominated flow for each time step. A current-dominated flow is required in order to make sure that wake shielding effects from the upstream cylinder always act on the downstream cylinder when subjected to a combined current plus waves.

Based on the above definition, the drag forces are updated at each time step based on the instantaneous relative distance x. The equation of motion becomes a high non-linear equation due to the position-dependent $C_D(x)$ and $V_r(x)$, and can be solved numerically by using the numerical time integration. A simplified method, as a first approximation, is to use a constant C_D based on the relative distance between cylinders obtained from static equilibrium position. It implies that the wake effect generated by the relative motion due to wave loads is neglected. In the following calculation, both the updated C_D and constant C_D will be applied and compared.

4.2. Current plus regular waves

The effect of the wake interference due to current plus regular waves is investigated in this section. The cylinders are placed at a submerged depth of $z = -60$ m, which is chosen because it represents a region where the relative distance was minimum according to the pre-

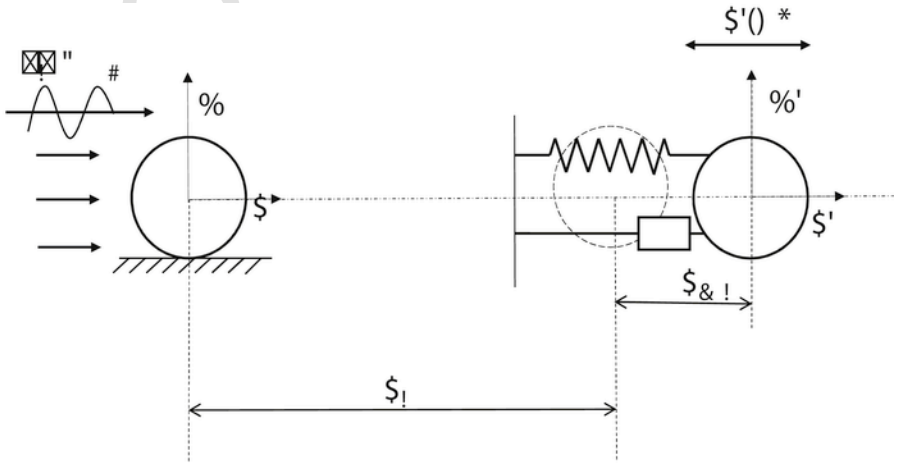

Fig. 10. Dynamic position of one degree-of-freedom downstream cylinder subjected to combined current-wave loading.

vious static analysis (in Section 2). Both cylinders have the same diameter $D = 0.25$ m. In order to apply the most critical environmental loads, the current and the waves are both taken to act in the x-direction. In Figs. 11–14, the calculated dynamic responses obtained by using both of the modified models are presented, with the frequency ratio defined as $\beta = \omega_w/\omega_n$ which varies from 0.6 to 1.4.

The surface wave elevation is $\zeta = \zeta_0 \sin(\omega_w t - kx)$, where ζ_0 is the wave amplitude, $\omega_w = 2\pi/T$ is the wave frequency and T is the wave period. Linear wave theory is used to calculate the wave particle velocity at a given water depth, i.e. $V_w = \omega\zeta_0 e^{kz}\cos(\omega_w t - kx)$, where the wave number is $k = 2\pi/\lambda$, and λ is the wave length determined from the deep water dispersion relationship, i.e. $\lambda = 2\pi g/\omega_w$. The natural frequency of the cylinder is $\omega_n = 2\pi/T_n = \sqrt{k_x/(m + m_a)}$ where T_n is the natural period of the cylinder.

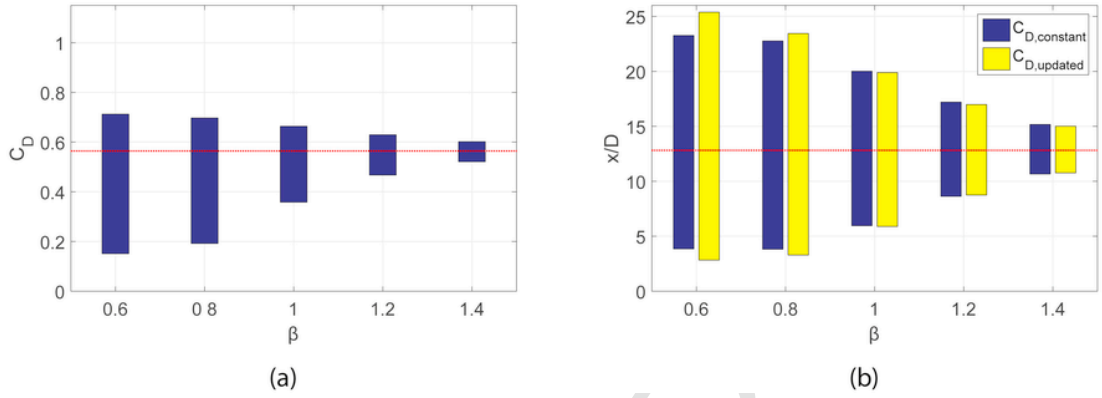

Fig. 11. Comparison of the downstream cylinder response for different frequency ratios by using the Blevins model, with $L_0 = 8D$. (a): The range of the corresponding $C_{D,constant}$ and $C_{D,updated}$. (b): The range of the displacement.

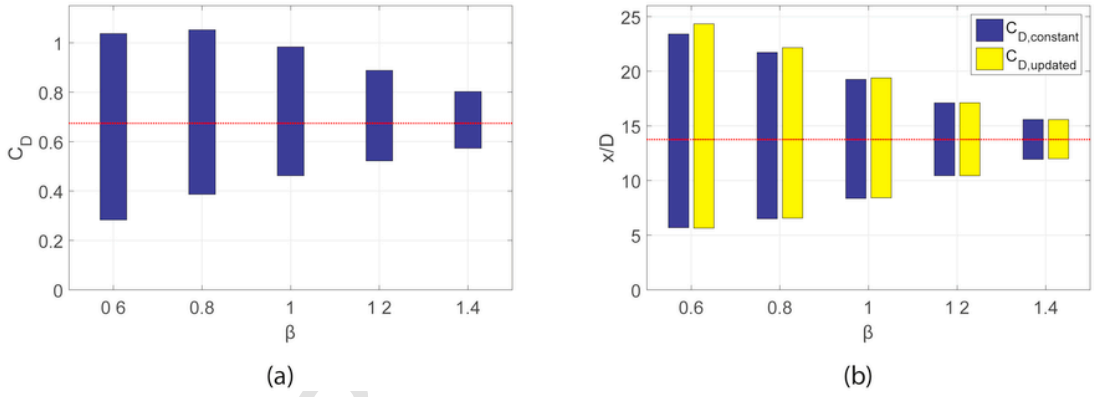

Fig. 12. Comparison of the downstream cylinder response for different frequency ratios by using the Huse model, with $L_0 = 8D$. (a): The range of the corresponding $C_{D,constant}$ and $C_{D,updated}$. (b): The range of the displacement.

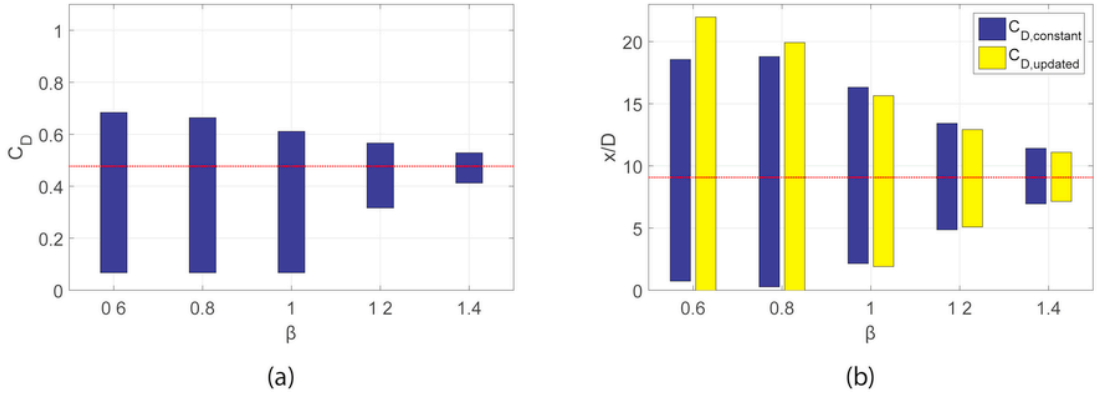

Fig. 13. Comparison of the downstream cylinder response for different frequency ratios by using the Blevins model, with $L_0 = 5D$. (a): The range of the corresponding $C_{D,constant}$ and $C_{D,updated}$. (b): The range of the displacement.

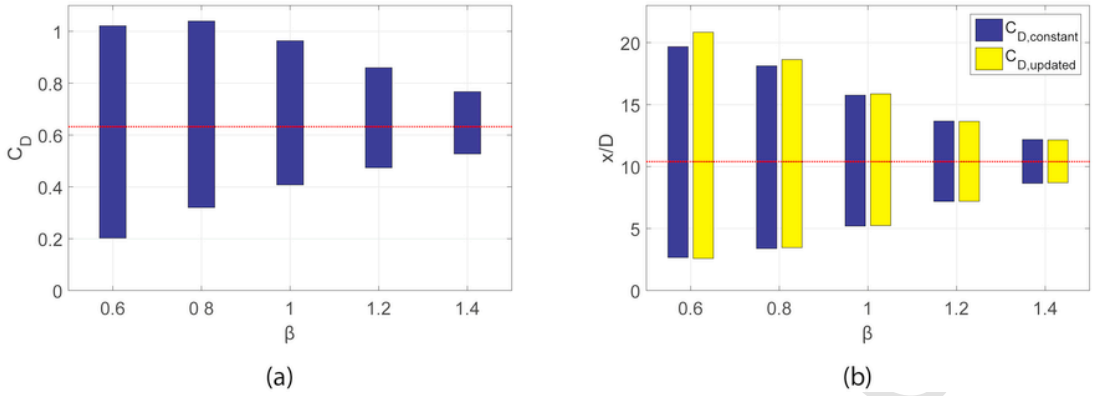

Fig. 14. Comparison of the downstream cylinder response for different frequency ratios by using the Huse model, with $L_0 = 5D$. (a): The range of the corresponding $C_{D,constant}$ and $C_{D,updated}$. (b): The range of the displacement.

The red dashed line in all figures indicates the static result when the risers are subjected to current only. Table 2 shows the prescribed cylinder and environmental conditions that are applied in the present study.

Fig. 11 shows the results obtained by application of the Blevins model for different values of the frequency ratio β. Both the results calculated from constant C_D and updated C_D, denoted as $C_{D,constant}$ and $C_{D,updated}$ respectively, are shown in the same figure. The initial distance is set to be $L_0 = 8D$. Fig. 11a illustrates the $C_D(x)$ range based on the calculations, and Fig. 11b shows the associated displacement range in terms of the non-dimensional displacement x/D for both $C_{D,constant}$ and $C_{D,updated}$.

From Fig. 11 it appears that, for results based on both $C_{D,constant}$ and $C_{D,updated}$, the cylinder moves to its static equilibrium position $x_r = 12.8D$ with the corresponding $C_D(x_r) = 0.56$ when subjected to the current loads. Subsequently, it oscillates around this position due to the wave loads. The amplitude of the motion is reduced as β increases. Apparently, this is because a small β corresponds to a long wave which induces a large particle motion amplitude. By comparing the amplitude of the motion calculated based on $C_{D,constant}$ and $C_{D,updated}$, it is found that the cylinder motion range is enlarged by using $C_{D,updated}$ for $\beta = 0.6$ and 0.8. This is because the drag force will increase due to the increase of the updated drag coefficient when the cylinder moves away from the upstream cylinder. Conversely, the drag coefficient will decrease when the cylinder moves towards to the upstream cylinder. However, as β increases, the importance of the drag force is reduced relative to the inertia force, so that the variation of the drag force will have an insignificant effect on the excitation force, accordingly also on the response of the cylinder.

Fig. 12 presents the results obtained by using the Huse model. The results associated with both the constant and updated drag coefficients are presented as well. The ranges of x/D for different β are shown in Fig. 12b. The static equilibrium position is $x_r = 13.8D$ with the corresponding $C_D(x_r) = 0.67$ as seen in Fig. 12a, which are slightly larger than the results obtained by the Blevins model. For each β, the Huse model leads to a relative smaller motion amplitude and a larger relative distance between the two cylinders as compared with the Blevins model, so that the collision probability will decrease. By comparing the results calculated based on $C_{D,constant}$ and $C_{D,updated}$, it is found that for the longer waves corresponding to $\beta = 0.6$ and 0.8, the maximum distance between the two cylinders is enlarged when using $C_{D,updated}$, while the minimum distance is almost the same. This implies that updating of the drag coefficient for the Huse model doesn't influence the dynamic response of the cylinder significantly. Similarly, the drag force becomes relatively less important as β increases, and accordingly the variation of the drag force has a limited effect on the excitation force, as well as on the response of the cylinder.

Table 2
Cylinder geometry and environment loading.

	Unit	Value
Cylinder diameter D	[mm]	250
Cylinder natural period T_n	[s]	15
Current velocity V_0	[m/s]	1.0
Wave height H	[m]	10.25
Frequency ratio β	[−]	[0.6, 0.8, 1, 1.2, 1.4]

Figs. 13 and 14 show the results obtained by application of the two modified models for an initial distance $L_0 = 5D$. For such a close initial distance, the cylinders are more likely to collide when subjected to current plus waves. According to the previous definition, collision events occur when the relative distance is $x_r < 2D$, and the drag coefficient of the downstream cylinder is here then locked at $C_D(x) = C_D(2D)$. As shown in Fig. 13, collisions occur both by applying $C_{D,constant}$ and $C_{D,updated}$ for $\beta = 0.6$,0.8 and 1.0 due to the low drag force when the cylinder moves towards to the upstream direction. As β increases $C_{D,updated}$ leads to a relatively small change in the motion amplitude since the hydrodynamic force is governed by the inertial force. Similarly, Fig. 14 shows the dynamic responses obtained by application of the Huse model. No collision is detected for the present condition, and the minimum distance between the two risers is not significantly affected by updating versus keeping the drag coefficient constant.

4.3. Current plus irregular waves

The wake effects on the downstream cylinder subjected to a combination of irregular waves and collinear current is studied in this section. The JONSWAP spectrum with a γ factor of 3.3 is used to characterize a sea state with significant wave height $H_s = 10.25$ m and peak period $T_p = 15$ s. The current velocity is $V_0 = 1m/s$. The duration of the simulation is 1 h for all the calculations. Fig. 15 show sequences of the time history of x/D for the downstream cylinder by application of the modified models for the initial distance $L_0 = 8D$. The green line indicates the collision event, i.e. $x = 2D$. The displacement histories of the cylinder from time $t = 2200$ s to $t = 2500$ s, which are obtained

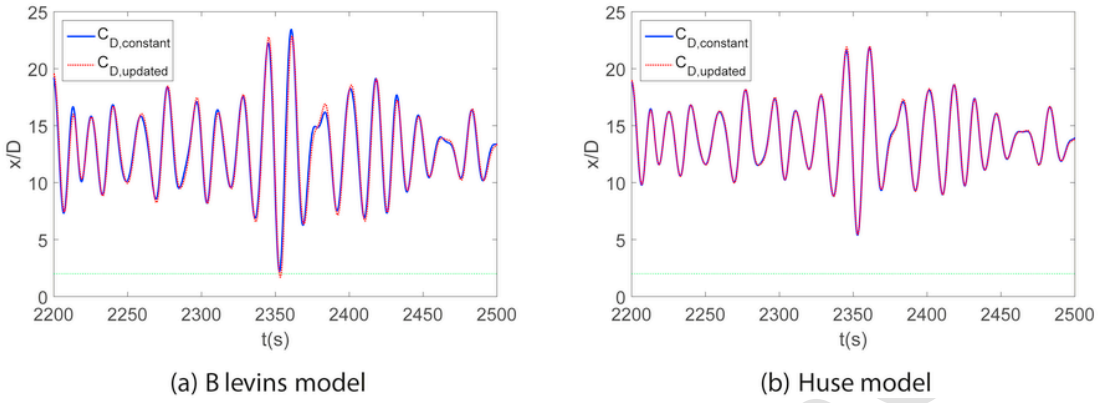

Fig. 15. Displacement time history of the downstream cylinder in random waves by using the Blevins model. (a): The Belvins model. (b): The Huse model.

by using the Blevins model based on both $C_{D,constant}$ and $C_{D,updated}$, are plotted in Fig. 15a. It appears that at $t = 2355$ s, the minimum distance is $x/D = 2.2$ for $C_{D,constant}$, and $x/D = 1.7$ for $C_{D,updated}$. A collision event is hence detected in the latter case. Similar results are plotted in Fig. 15b by application of the Huse model, and no collision is detected by application of both sets of drag coefficients. Based on the comparison of these results it is found that the Blevins model will imply a relatively higher risk of collision than the Huse model.

5. Collision probability

The collision probability associated with random waves is further considered. The probability of the riser collision, actually, is an extreme minimum value problem. It is convenient to transform the extreme minimum value problem to the extreme maximum value problem in non-dimensional form by writing the process as:

$$X(t) = -\frac{x}{D} \tag{10}$$

In this way, $X(t) < 0$, and the cylinders physically collide when $X(t) \leq -1$. In the present study, however, it is defined that the collision occurs when $X(t) \leq -2$ based on the previous discussion.

Due to the statistical uncertainties which are inherent in the random response process, repeated simulations are required in order to obtain a reliable estimation of the extreme response. The classical extreme value theory assume that the distribution of a sequence of independent and identically distributed random variables will normally converge towards one of three possible asymptotic extreme value distributions as $n \to \infty$ (Naess and Moan, 2012). In the present study, the Gumbel distribution function will be adopted due to the behaviour of the upper tail of the distribution of maxima. The Gumbel probability paper method is a simple and efficient method to determine the distribution parameters. The cumulative distribution function is given by:

$$F_{X_e}(x) = \exp\{-\exp(-\alpha(x-u))\} \tag{11}$$

where α and μ are the scale and location parameters, respectively. By taking the logarithm of both left and right hand side of this equation twice, the following equation is obtained:

$$-\ln\left[-\ln\left(F_{X_e}(x)\right)\right] = \alpha(x-u) \tag{12}$$

Further, by introducing $y = -\ln[-\ln(F_{X_e}(x))]$ a linear function $y = \alpha(x-u)$ is obtained, which implies that in a x-y axis system, the cumulative distribution becomes a straight line. The parameters α and μ can be estimated by the least-square fitting of the samples to the straight line.

The fitted straight line and the extreme samples identified from the 25 1-h simulations with different random seeds for generating time series of waves are plotted in Figs. 16 and 17, with the Blevins model and Huse model, respectively. The results obtained by application of the constant and updated $C_D(x)$ are plotted in the same figure for each model. The failure criterion, i.e., $X \geq -2$ is illustrated as the dotted vertical line. The estimated Gumbel parameters and the failure proba-

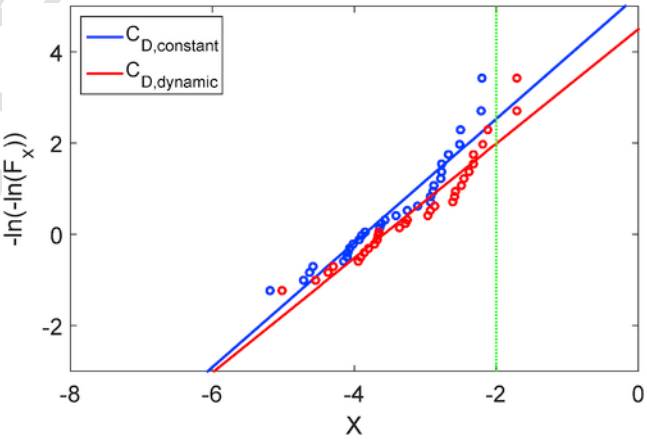

Fig. 16. Gumbel probability paper with the samples of minimum distance for the Blevins model with $L_0 = 8D$.

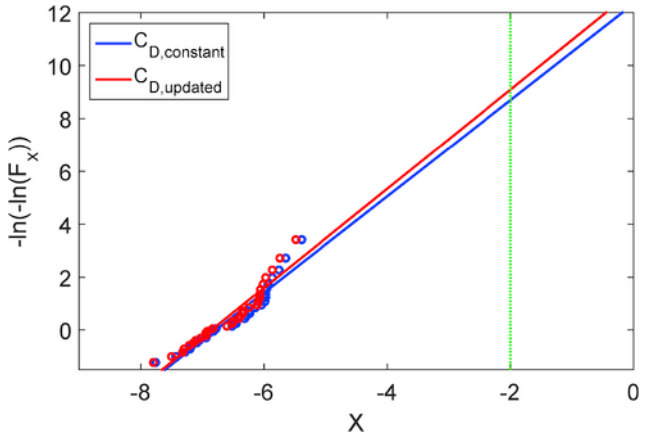

Fig. 17. Gumbel probability paper with the samples of minimum distance for the Huse model with $L_0 = 8D$.

bility $P_f = 1 - F_X$ obtained by the two models are summarized in Table 3.

Generally, the results show that the Blevins model increases the probability of failure by about two orders of magnitude, thus emphasizing the importance of accounting for the uncertainties related to the wake model in the context of a riser collision reliability assessment. It is also found that updating of C_D has a noticeable effect on the probability of failure for the present case with $\beta = 1$ for the Blevins model. This implies that the uncertainties of the value of C_D must be estimated before a proper collision reliability assessment can be performed. On the contrary, the results obtained by using the Huse model imply that the uncertainties of the value of C_D is less important.

6. Conclusions

Consideration of the wake interference in the near field is essential for prediction of the likelihold of riser collision. In Fu et al. (2017) a method for this purpose was proposed. However, in that study, only the wake interaction based on the static Blevins model was considered.

In the present work, an additional modified wake model in the near field, i.e. the Huse model, is presented together with the Blevins model, and the results from both models are compared. The effect of the wake on the static deflection of a pair of flexible risers is studied by using the computer code Riflex for both the modified models. The results identify the region where the risers are most likely to collide, and some modifications of the riser system in order to avoid collision are proposed.

Waves can also cause riser collision if the wave-induced loading is sufficiently large to cause the risers to interact. Therefore, wake interference in waves is investigated based on the assumption that the modified wake models, which were established for steady flow conditions, can also be applied for current-dominated flow for each time step. By comparing this dynamic wake model with the static model, it is found that the effect of $C_{D,updated}$ depends on the frequency ratio β.

For a 'No Collision Allowed' approach to design of marine risers, the collision failure event is regarded as an extreme value problem. By using a Gumbel probability paper, it is found that the uncertainties associated with the wake model has a significant effect on the failure probability estimation. As a general observation, it is found that these model uncertainties must be properly reflected in order to perform an adequate reliability assessment.

Table 3
Estimated parameters of Gumbel distribution function and failure probability.

Models	$C_{D,constant}$			$C_{D,updated}$		
	α	μ	P_f	α	μ	P_f
Blevins	1.36	−3.86	7.65×10^{-2}	1.25	−3.58	1.28×10^{-1}
Huse	1.82	−6.78	2.00×10^{-4}	1.87	−6.85	1.00×10^{-4}

References

Blevins, R., 2005. Forces on and stability of a cylinder in a wake. J. Offshore Mech. Arct. Eng. 127 (1), 39–45.

Bokaian, A., Geoola, F., et al., 1985. Hydrodynamic forces on a pair of cylinders. In: Offshore Technology Conference. Offshore Technology Conference.

Bushnell, M., et al., 1977. Forces on cylinder arrays in oscillating flow. In: Offshore Technology Conference. Offshore Technology Conference.

DNV-RP-F203, 2009. Offshore Standard Dnv-rp-f203: Riser Interference. Det Norske Veritas, Norway.

Duggal, A.S., Niedzwecki, J.M., 1993. Regular and Random Wave Interaction with a Long Flexible cylinder.

Fredheim, A., 2005. Current Forces on Net Structure.

Fu, P., Leira, B.J., Myrhaug, D., 2017. Reliability analysis of wake-induced collision of flexible risers. Appl. Ocean Res. 62, 49–56.

Herfjord, K., Holmas, T., Leira, B., Bryndum, M., Hanson, T., 2002. Computation of interaction between deepwater risers: collision statistics and stress analysis. In: ASME 2002 21st International Conference on Offshore Mechanics and Arctic Engineering. American Society of Mechanical Engineers, pp. 299–305.

Hover, F.S., Triantafyllou, M.S., 2001. Galloping response of a cylinder with upstream wake interference. J. Fluids Struct. 15 (3), 503–512.

Huang, S., Herfjord, K., 2013. Experimental investigation of the forces and motion responses of two interfering viv circular cylinders at various tandem and staggered positions. Appl. Ocean Res. 43, 264–273.

Huang, S., Khorasanchi, M., Herfjord, K., 2011. Drag amplification of long flexible riser models undergoing multi-mode viv in uniform currents. J. Fluids Struct. 27 (3), 342–353.

Huera-Huarte, F., Bearman, P., 2011. Vortex and wake-induced vibrations of a tandem arrangement of two flexible circular cylinders with near wake interference. J. Fluids Struct. 27 (2), 193–211.

Huera-Huarte, F., Gharib, M., 2011. Vortex-and wake-induced vibrations of a tandem arrangement of two flexible circular cylinders with far wake interference. J. Fluids Struct. 27 (5), 824–828.

Huse, E., Kleiven, G., Nielsen, F.G., 1998. Large scale model testing of deep sea risers. In: Offshore Technology Conference.

Huse, E., Kleiven, G., Nielsen, F.G., 2000. Impulse and energy in deepsea riser collisions owing to wake interference. In: Offshore Technology Conference.

Naess, A., Moan, T., 2012. Stochastic Dynamics of marine Structures. Cambridge University Press.

Price, S., Paidoussis, M., 1984. The aerodynamic forces acting on groups of two and three circular cylinders when subject to a cross-flow. J. Wind Eng. Ind Aerod. 17 (3), 329–347.

RIFLEX, 1987. Review of Flow Interference between Two Circular Cylinders in Various Arrangements. Theory Manual.

Schlichting, H., Gersten, K., 2003. Boundary-layer Theory. Springer Science & Business Media.

Wu, W., 2003. Interaction between Two marine Risers. Ph.D. thesis University of Glasgow.

Zdravkovich, M., 1977. Review of flow interference between two circular cylinders in various arrangements. J. Fluids Eng. 99 (4), 618–633.